UC Irvine
UC Irvine Previously Published Works

Title
Nonlinear Optical Corneal Crosslinking, Mechanical Stiffening, and Corneal Flattening Using Amplified Femtosecond Pulses.

Permalink
https://escholarship.org/uc/item/9zh7d4rw

Journal
Translational vision science & technology, 8(6)

ISSN
2164-2591

Authors
Bradford, Samantha
Mikula, Eric
Kim, Sun Woong
et al.

Publication Date
2019-11-01

DOI
10.1167/tvst.8.6.35

Peer reviewed

Article

Nonlinear Optical Corneal Crosslinking, Mechanical Stiffening, and Corneal Flattening Using Amplified Femtosecond Pulses

Samantha Bradford[1],*, Eric Mikula[1],*, Sun Woong Kim[1,2], Yilu Xie[1], Tibor Juhasz[1], Donald J. Brown[1], and James V. Jester[1]

[1] University of California, Irvine, Department of Ophthalmology and Biomedical Engineering, Irvine, CA, USA
[2] Yonsei University, Wonju College of Medicine, Department of Ophthalmology, Wonju, South Korea

Purpose: We have shown that nonlinear optical corneal crosslinking (NLO CXL) and stiffening can be achieved in ex vivo rabbit corneas using an 80-MHz, 760-nm femtosecond (FS) laser, however the required power was beyond the American National Standard Institute limit. The purpose of this study was to test the efficacy of amplified FS pulses to perform CXL to reduce power by increasing pulse energy.

Methods: A variable numerical aperture laser scanning delivery system was coupled to a 1030-nm laser with a noncollinear optical parametric amplifier to generate 760 nm, 50 to 150 kHz amplified FS pulses with 79.5-μm axial and 2.9-μm lateral two-photon focal volume. Ex vivo rabbit corneas received NLO CXL, and effectiveness was assessed by measuring collagen autofluorescence (CAF) and mechanical stiffening. NLO CXL was also performed in 14 live rabbits, and changes in corneal topography were measured using an Orbscan.

Results: Amplified pulses (0.3 μJ) generated significant CAF that increased logarithmically with decreasing scan speed; achieving equivalent CAF to UVA CXL at 15.5 mm/s. Indentation testing detected a 62% increase in stiffness compared to control, and corneal topography measurements revealed a significant decrease of 1.0 $\pm$ 0.8 diopter by 1 month ($P < 0.05$).

Conclusions: These results show that NLO CXL using amplified pulses can produce corneal collagen CXL comparable to UVA CXL.

Translational Relevance: NLO CXL using amplified pulses can produce corneal CXL comparable to UVA CXL, suggesting a potential clinical application in which NLO CXL can be used to perform personalized crosslinking for treatment of refractive errors and keratoconus.

Introduction

Myopia is the most common refractive error and is estimated to affect 1.6 billion people worldwide, with a prevalence of 33% in the United States and up to 80% to 90% in East Asian young adults.[1,2] Since its introduction nearly 30 years ago, laser-assisted in situ keratomileusis (LASIK) has become the standard of care for surgical correction of refractive errors.[3] The procedure entails cutting a corneal flap and ablating the stroma underneath with an excimer laser, thus modifying corneal curvature to better focus light back onto the retina. Despite high patient satisfaction rates of LASIK (>95%),[4] many patients, such as those with thin corneas, suspected keratoconus, or those with mild refractive errors, are not ideal candidates for the procedure. Specifically, in patients with low refractive error ($\pm$2 diopters), the risks associated with cutting the LASIK flap may outweigh the benefits of a successful surgery. These patients can typically function day to day uncorrected, opting to wear glasses only during certain activities such as driving. This creates an unmet medical need for a noninvasive,

safer procedure for the correction of low refractive errors.

In recent years, a number of technologies have emerged with the potential to address the issue of a safer, less-invasive refractive surgery for low refractive errors by avoiding cutting of a flap. The first technology in this category, ultraviolet A (UVA) corneal collagen crosslinking (CXL), was initially developed in the early 2000s as a treatment for keratoconus, but it has been increasingly investigated as a refractive procedure.[5,6] UVA CXL uses UVA light to photoactivate riboflavin (previously imbibed into the stroma via eye drops), thus generating an excited triplet state of riboflavin, free oxygen radicals, and subsequent crosslinking of collagen fibrils. With respect to keratoconus, the goal of CXL is to halt the progression of the disease by strengthening the cornea. In regard to potential refractive CXL, the goal is to selectively alter the biomechanical properties of the corneal stroma via collagen crosslinks, thereby changing the topography of the cornea and correcting vision.

While UVA CXL is the most commonly used method to achieve corneal CXL, the use of femtosecond (FS) lasers has also gained interest in recent years. Wozniak et al.[7] utilized blue (480 nm) FS pulses to induce a refractive index change in corneal tissue, while Wang et al.[8] reported corneal CXL without riboflavin using infrared pulses. The nature of these two methods, however, is not directly based on the original UVA CXL methodology, and therefore explanations of the principles underlying these techniques are not fully understood. Our group has previously used an 80 MHz FS laser oscillator tuned to 760 nm to crosslink corneal collagen via nonlinear two-photon excitation of riboflavin, a technique referred to as nonlinear optical collagen crosslinking (NLO CXL).[9–11] NLO CXL uses two photons of near infrared FS laser light (with a combined energy of one UVA photon) to excite riboflavin, thus generating oxygen free radicals and subsequent collagen crosslinking, similar to UVA CXL. However, this technique is distinctly different from UVA CXL in that the excitation of riboflavin, and thus crosslinking, only occurs in the well-defined and specifically chosen two-photon focal volume of the laser delivery objective. The location of the focal volume can be arbitrarily scanned with micrometer precision to achieve a crosslinking area of any geometry and depth within the cornea. While we achieved corneal CXL and mechanical stiffening on par with UVA CXL, these studies used a high repetition rate (80 MHz) low-pulse energy (10 nJ) laser requiring a high average power (~800 mW), well above the American National Standards Institute (ANSI) limit of 46.1 mW.[12]

To address this issue and reduce the average power exposure to a clinically acceptable level, this study explored using regeneratively amplified FS laser pulses (microjoule pulse energy) at low repetition rates (kilohertz) to precisely crosslink corneal collagen while remaining under the ANSI limit of 46.1 mW. By increasing pulse energy from 10 nJ to 1 µJ, it was expected that the average total energy could be proportionally reduced from 800 to 8 mW. This was verified in ex vivo eyes after treatment with a 5 kHz amplified FS laser using the presence of collagen autofluorescence (CAF) as an indicator that CXL had occurred.

Following preliminary experiments using 1-µJ pulse energies, a custom noncollinear optical parametric amplifier (NOPA) was designed and built to deliver 760 nm amplified FS laser pulses at repetition rates of 50 to 150 kHz. Amplified NLO CXL was performed in ex vivo rabbit eyes, after which collagen autofluorescence and mechanical stiffness measurements were performed. Crosslinking experiments were also carried out in live rabbits, and topography was measured to assess refractive outcomes of amplified NLO CXL.

Methods

Proof of Concept

Prior to building a custom amplified NLO CXL system, the question of whether NLO CXL was even possible using amplified FS pulses was determined by examining CAF within ex vivo rabbit eyes treated by coupling our delivery optics with an amplifier system (Legend-F Titanium Sapphire Regenerative Amplifier; Coherent, Inc., Santa Clara, CA). This 5-kHz, 130-FS, 800-nm laser light was directed through an optical parametric amplifier (OPA) (Opera-LE-F OPA; Coherent, Inc.) to produce 1520-nm laser light that was then frequency doubled using a beta barium borate (BBO) crystal to produce a 760-nm beam with 1-µJ pulse energy. FS pulses were then focused into our previously described delivery device that uses a patented, low numerical aperture focusing system to generate enlarged two-photon volumes of 2 to 3 µm in diameter and 100 µm in axial length, as previously described.[10,11]

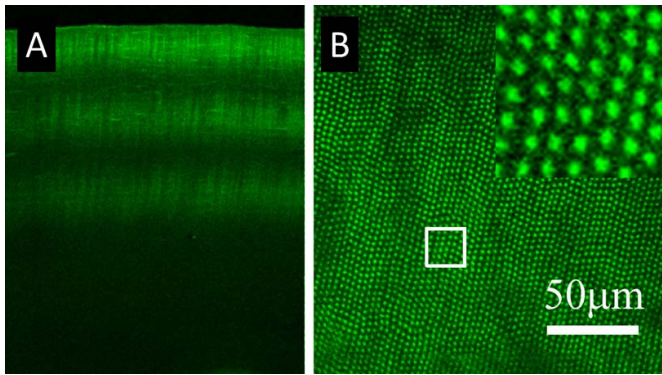Using the 5-kHz repetition rate, ex vivo rabbit

Figure 1. CAF of single spot amplified NLO CXL. The image shown in (A) demonstrates the CAF within a vibratome section of a cornea treated with three separate layers of single spot amplified NLO CXL. (B) The en face view of a cornea treated in the same way. A grid of CAF spots can clearly be seen within the sample, and each spot represents CXL from a single amplified pulse.

corneas were raster scanned over a 4-mm-diameter area at a scan speed of 15 mm/s to produce single pulse, 2- to 3-μm-diameter CAF spots with a 3-μm spot separation using a total power of only 5 mW. Corneas were then removed from the eye and fixed in 2% paraformaldehyde (PFA) in PBS, pH 7.2, overnight prior to two-photon detection of corneal CAF using a multiphoton confocal microscope (Zeiss 510; Carl Zeiss, Jena, Germany) and FS laser (Chameleon; Coherent, Inc.) as previously described.[10,11,13] Briefly, the presence of CAF was detected using 760-nm FS laser light to induce two-photon excited blue light 400- to 450-nm CAF from crosslinked regions of the cornea. CAF was examined within both vibratome cross sections and whole mount corneas viewed en face or parallel to the corneal surface (Fig. 1). Similar tissue preparation and imaging were performed for detection of CAF in later studies. The presence of CAF within these samples was used as justification for building a more stable system with a higher repetition rate, able to crosslink at faster speeds.

Amplified FS Laser and Delivery

Though commercially available FS oscillators are broadly tunable and can readily deliver 760-nm FS laser pulses, commercial turnkey amplified FS laser systems are not available at this wavelength. However, photons of different wavelengths can be generated from an FS laser source using nonlinear processes in an OPA. In this study, we used a commercially available amplified FS laser operating at 1030 nm (One Five Origami; NKT Photonics, Birkerod, Den-

mark), with a variable repetition rate (50–150 kHz), 318-FS pulse duration, and 4-W average power as the laser source for a lab-built NOPA. The NOPA generated variable microjoule pulses of 760-nm FS light, which were then aligned into the beam delivery/scanning device from our previous study[10] and then into the eye. An overview of the entire system is presented in Figure 2. In general, a NOPA is a device capable of converting a pump photon of a specific wavelength into two photons of longer wavelengths, termed signal and idler. The wavelengths of the signal and idler can be continuously tuned as long as the requirement of energy conservation is met. The NOPA built for this study contains three stages: supercontinuum generation, formation of the pump beam, and parametric conversion.

Stage 1: Supercontinuum Generation

Approximately 10% of the output of the 1030-nm laser source is picked off by a beam splitter and focused onto a 200-μm-thick sapphire plate (Fig. 2, stage 1). Acting as a nonlinear medium, this spectrally broadens the original laser pulse via self-phase modulation, creating supercontinuum radiation that appears like white light to the eye. Centered at 1030 nm, the supercontinuum radiation contains spectral components from 500 to 1500 nm. The output is well-formed and smoothly varying, making it a suitable source to serve as the "seed" pulse for the OPA. The white light is passed through two water cuvettes, adding group velocity dispersion to the supercontinuum and ultimately reducing the bandwidth of the 760-nm OPA output to 12 nm.

Stage 2: Pump Formation

After the 10% beam splitter, the remaining 1030-nm source beam is sent to a 2-mm-thick BBO crystal for frequency doubling (Fig. 2, Stage 2). The 2-mm BBO is responsible for converting the source from 1030 to 515 nm, which can then be used to generate the two longer wavelength photons in the visible spectrum. BBO is used due to its large second-order susceptibility, χ^2, as well as its high damage threshold.

Stage 3: Parametric Conversion

After frequency doubling in stage 2, the 515-nm radiation is sent to a second 400-μm-thick BBO crystal (Fig. 2, stage 3) for parametric conversion. After passing through the second BBO crystal, the 515-nm light produces a parametric ring of visible radiation. As the crystal angle is varied, color separation can be observed within the ring. The proper crystal angle is determined by finding the angle

Figure 2. Custom NOPA schematic. Schematic shows the components of the amplified NLO CXL device. The device consists of three main elements: (1) The laser source (OneFive regeneratively amplified FS laser) produces 1030 nm amplified FS pulse light. (2) The NOPA consisting of three stages (supercontinuum generation, frequency-doubled pump beam generation, and parametric conversion) is used to alter the wavelength of the input beam to 760 nm. (3) The laser delivery system focuses the resulting 760 nm amplified FS light into the eye. Amplified FS light is directed through the three NOPA stages using a series of mirrors (*M*) and specified focal length lenses (*f*), through a dispersion compensation prism pair (DCP) for pulse compression, and then into the delivery optics.

that minimizes color separation. Once this angle is found, the supercontinuum seed from stage 1 is spatially overlapped with the 515-nm pump in the second BBO crystal and directionally overlapped with the parametric ring. After this is accomplished, the translation stage shown in Figure 2 (delay 1) is adjusted to ensure proper temporal overlap between the seed pulse and the 515-nm pump pulse. When both the seed and pump pulses are aligned spatially, directionally, and temporally, the parametric ring of radiation collapses into a beam that takes on the properties of the original pump beam. Owing to the fact that the supercontinuum seed is chirped, wavelength tuning can be accomplished by altering the timing of the seed relative to the pump pulse by adjusting delay 2 (Fig. 2). For this study, the center wavelength of the NOPA was adjusted to 760 nm with a full width at half maximum (FWHM) bandwidth of 12 nm, as measured by a spectrometer (Thorlabs, Newton, NJ). The pulse duration of the newly formed 760-nm beam was measured using a lab-built autocorrelator and found to be ∼700 FS. The beam is then passed twice through an SF10 ultrafast laser dispersion compensation prism pair (DCP 1 and 2), which has the effect of compressing the pulse and thus controlling pulse duration. After compression, the pulse duration was measured to be ∼400 FS.

Laser Delivery

Upon leaving the pulse compressor, the beam passes through a half wave plate ($\lambda/2$) and polarizing beam cube that function as a continuously variable beam attenuator. The rest of the beam delivery optics are identical to those used in our previous study.[10] Briefly, the beam passes through a variable expanding telescope before entering a series of galvo steering mirrors that together scan the beam in a preprogrammed raster pattern at a preprogrammed speed. The beam then passes through a second expanding telescope before being directed down into the objective and through the applanation glass and into the cornea. The effective numerical aperture of the delivery system used in this study was 0.12, which would theoretically result in a focal volume with axial and lateral dimensions of 79.5 and 2.9 μm, respectively, as calculated using Zipfel's equations.[14]

Amplified NLO CXL in the Ex Vivo Rabbit Cornea

After confirming crosslinking using amplified FS pulses was possible, it was necessary to determine the amount of amplified FS pulse energy needed to achieve corneal crosslinking at levels equal to standard UVA CXL. The amount of energy deposi-

Table 1. Scan Speed and Total Energy

Scan Speed, mm/s	Group Size, n	5-μm Line Spacing[a]		2-μm Line Spacing[a]	
		Treatment Duration, min	Total Energy, J	Treatment Duration, min	Total Energy, J
100	3	0.53	0.96	1.33	2.4
80	3	0.67	1.2	1.67	3.0
60	3	0.89	1.6	2.22	4.0
40	3	1.33	2.4	3.33	6.0
30	4	1.64	2.96	4.11	7.4
20	6	2.66	4.8	6.66	12.0
10	3	4.93	8.88	12.33	22.2
5	4	9.86	17.76	24.66	44.4
UVA CXL	NA	NA	NA	30	5.4

[a] Line separations of 5 μm were used for CAF analysis, whereas 2-μm separations were used for mechanical testing. All NLO CXL treatments were performed over a 4-mm-diameter area.

tion was controlled by varying the scan speed of the laser beam and thus the amount of laser pulses per unit area along the scan line. Previously, our group, as well as others, has used CAF as a metric to assess the degree of collagen crosslinking.[9–11,15–17] The same method was used in this study, with CAF being compared against our previously published CAF data using standard UVA CXL.[13] After a suitable scan speed was determined, we performed mechanical testing to determine the effect of amplified NLO CXL on tissue stiffness.

Scan Speed Versus CAF

A total of 29 rabbit eyes were shipped overnight on ice (Pel-Freez Biologicals, Rogers, AR); experiments were performed the same day as delivery. The epithelium was mechanically removed in the central 8 mm of the cornea with a Tooke knife. The corneas were then imbibed with riboflavin via eye drops containing 0.5% riboflavin-5-phospate and 20% high fraction dextran, molecular weight 450 to 650 kDa (Sigma-Aldrich Corp., St. Louis, MO) in PBS solution once every 2 minutes for 30 minutes. Next, the eyes underwent amplified NLO CXL in the central 4 mm of the cornea. Treatment groups were defined by the scan speed of the laser beam, ranging from 5 to 100 mm/s. The beam was scanned in a single plane in a raster pattern as described previously, with a line separation of 5 μm to shorten the scanning time required for this portion of the study.[10,11] The depth of focus was set for 50 μm below the contact glass so as to include the entire focal volume within the tissue. The pulse energy and average power were set to 0.3 μJ and 30 mW, respectively, at 50- to 100-kHz pulse

repetition frequency, well beneath the ANSI limit of 46.1 mW. The parameters for each treatment group as well as each group size are outlined in Table 1. Each group had at least three eyes ($n = 3$). The treatment times reported in this table were calculated for line separations of both 2 and 5 μm, since the 5-μm separation used for CAF evaluation was later reduced to 2 μm for mechanical measurements and in vivo treatments. The values for standard UVA CXL are also provided for reference. After treatment, corneas were prepared for CAF measurements.

CAF was measured per the protocol in our previous studies, taking care to faithfully replicate the measurements via laser power and microscope settings to allow for reliable comparison.[10] Briefly, after amplified NLO CXL, corneas were excised from the globe and fixed overnight in 2% PFA (Mallinckrodit Baker, Inc., Phillipsburg, NJ) in PBS at 4°C. The corneas were then sectioned into 250-μm-thick slices perpendicular to the axis of crosslinking using a vibratome (Campden Instruments, Loughborough, England). The samples were then imaged for blue CAF using a microscope (Zeiss LSM 510; Carl Zeiss) and a Coherent FS laser as an excitation source. The samples were excited at 760 nm while the CAF signal was collected between 400 and 450 nm using a bandpass filter.

The images were exported to image analysis software (Metamorph; Molecular Devices, Sunnyvale, CA), and three 100×100 pixel areas within both the central anterior crosslinked region and the background region were identified. The average intensities within both regions were then subtracted. To compensate for the fact that line separation was
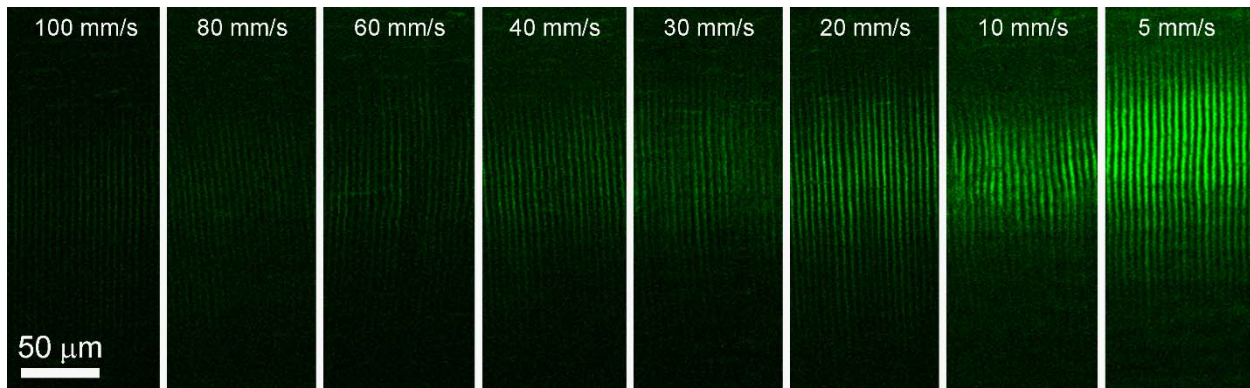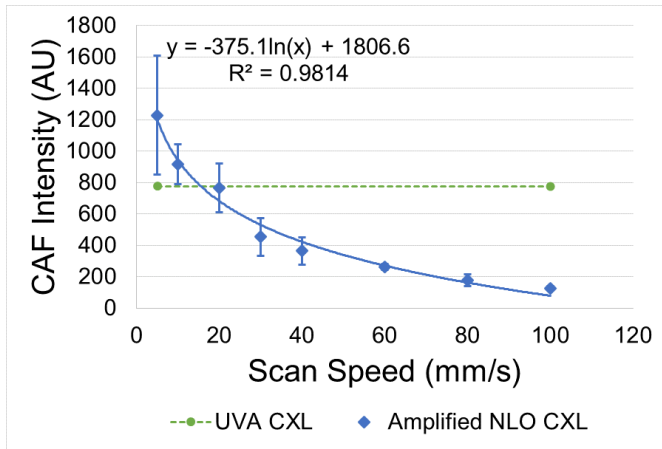
Figure 4. CAF intensity versus scanning speed. CAF intensity of amplified NLO CXL–treated eyes plotted with respect to increasing scanning speed and compared to CAF of previously reported UVA CXL data.[13] The data fit the line $y = -375.1 \ln(x) + 1806.6$ with an R^2 value of 0.9814 and intersected the UVA CXL CAF line at a speed of 15.5 mm/s. *Error bars* represent standard deviation.

to take the measurement. A minimum of three complete scans were made for each eye at each time point, Before all CMTF or topography procedures, animals were anesthetized using a subcutaneous injection of 30 to 50 mg/kg ketamine hydrochloride (Hospira, Irvine, CA) and 5 to 10 mg/kg xylazine (Akorn, Lake Forrest, IL). The effect of the procedure was measured by calculating the difference in refractive power, using a minimum of three measurements per exam, between the right and left eye at each time point (ΔD).

For amplified NLO CXL, sedated animals received a drop of topical ophthalmic 0.5% tetracaine hydro-chloride (Alcon, Ft. Worth, TX) to prevent pain. The methods for epithelial removal and stromal riboflavin delivery were identical to those used in the ex vivo experiments described above. The right eyes then underwent amplified NLO CXL in the central 4 mm with a 2-µm line separation using a pulse energy and average power of 0.3 µJ and 30 mW at a laser scan speed of 20 mm/s. After treatment, the rabbits received a subcutaneous 0.1 mL injection of buprenorphine hydrochloride (Reckitt Benckiser Healthcare Ltd., Slough, UK) for pain. For 3 days following the procedure, each rabbit received an antibiotic eye drop, 0.3% gentamicin sulfate (Allergan, Inc., Irvine, CA), three times daily in the treated eye to prevent infection. After either 2 weeks (five rabbits) or 8 weeks (nine rabbits) post treatment, animals were euthanized via an intravenous injection (Euthanasia III; Vedco, Inc., St. Joseph, MO) into the marginal ear vein after the last

topography measurement. Immediately after death, corneas were fixed in situ under 20 mm Hg pressure via perfusion of 2% PFA to maintain the in vivo collagen structure, as described in previous studies.[13] The corneas were then excised and prepared for CAF measurements in the same manner as described above for ex vivo eyes to confirm the presence of crosslinking. After CAF was examined, sections were stained with phalloidin (1:100) and ethidium homodimer (2 µL/mL) for fluorescent imaging of cellular structures as described in previous studies.[13]

Statistics

Statistical analysis was performed using the Tukey-Kramer method for a multiple comparison, 1-way or repeated measures analysis of variance in statistical software (MatLab; Mathworks, Natick, MA). Groups were considered to have a statistically significant difference with a P value of less than 0.05. In all figures, error bars represent standard deviation.

Results

Ex Vivo Amplified NLO CXL

Scan Speed Versus CAF Intensity

Examples of CAF images used for measurements are shown in Figure 3. The measured CAF intensities corresponding to each treatment speed are graphed in Figure 4. CAF intensity was scaled downward logarithmically with increasing scan speed and fit to the equation $y = -375.1 \ln(x) + 1806.6$ with an $R^2 = 0.9814$. Using the FWHM values from a line scan perpendicular through the crosslinked area of NLO CXL CAF images, the percentage of crosslinked area was measured to be 61.4%. Using Zipfel's equations,[14] a comparable theoretical value of 58% was calculated. UVA CXL CAF values reported in a previous study (1267 ± 181)[13] were converted to 777.9 ± 111.1, using this percentage to compensate for the spacing between scan lines in NLO CXL CAF images. Namely, only 61.4% of the UVA CXL CAF was considered. Using this value, amplified NLO CXL reached a comparable CAF intensity to UVA CXL at a speed of 15.5 mm/s.

Corneal Stiffness

The indentation elasticity values of corneas treated using amplified NLO CXL were measured to be 84.3 $\pm$ 5.9 kPa ($n = 4$), 1.62 times larger than control values that averaged 52.2 ± 8.6 kPa ($n = 5$). After
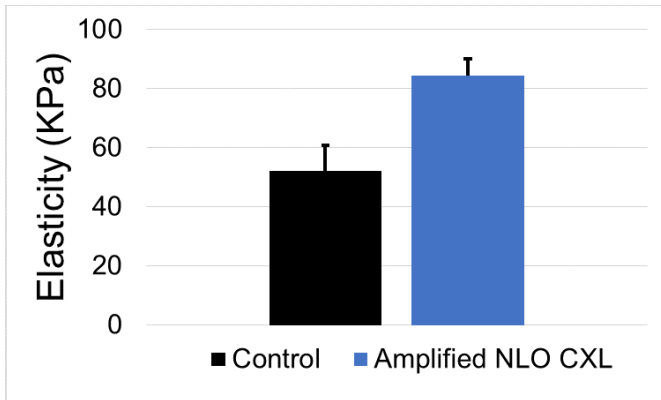
Figure 5. Elasticity after amplified NLO CXL. Amplified NLO CXL (*n* = 4) produced a 1.62-fold statistically significant increase in corneal elasticity compared to control corneas (*n* = 5) (*P* < 0.05). *Error bars* represent standard deviation.

statistical analysis, this difference was found to be statistically significant (*P* < 0.05). A comparison of these two values is provided in the graph in Figure 5.

In Vivo Amplified NLO CXL

Clinical observation of the corneas 48 hours after treatment revealed very little irritation of the tissue. No significant redness, swelling, or visible haze was observed, as can be seen in Figure 6A. Figure 6B and 6C show a cross-sectional CMTF image and a 178-μm deep plane image within a cornea at 2 weeks. The scattering seen in Figure 6B and the spindle-shaped cell bodies seen in Figure 6C indicate cellular migration within the treated region at 2 weeks. CMTF imaging within the short-term group also revealed a significantly thicker epithelium (42.4 ± 1.5 vs. 36.1 ± 1.8 μm), an unchanged stromal thickness (315.6 ± 23.7 vs. 310.6 ± 19.2 μm), and significantly increased haze (3148.1 ± 622 vs. 1303.1 ± 527) in the treated eye compared to control. Figure 6D shows CAF taken within a vibratome section after 2 weeks

of healing. A consistent 110-μm-thick band of CAF can be seen 90 μm below the surface of the epithelium. Furthermore, cellular staining using phalloidin and ethidium homodimer (Fig. 6E) revealed the presence of keratocytes within the treated region of all samples. This is noticeably different from the completely acellular region seen in samples treated with UVA CXL in previously reported studies.[13]

In the long-term group, corneal flattening was measured as the diopter difference (ΔD) of the central 3 mm between the right and left eye (R-L) of each rabbit prior to treatment and at the intervals listed previously. For this reason, a negative value indicates flattening of the treated eye. Corneal flattening was also measured as the ΔD of each cornea compared to baseline (ΔR or ΔL, respectively). Measurements of two rabbits were excluded because CAF could not be detected in the treated eye after sacrifice. Our previous studies have shown that CAF is unchanged even after 3 months of healing,[13] so the lack of any CAF was considered indicative of a lack of CXL. There are various reasons this error may have occurred. For example, the pupil may have been misaligned during treatment, or the rabbit may have slipped during the treatment. In either case, the treatment would not have been located in the center of the cornea and therefore was not measured in the correct location in subsequent testing. Example topography measurements of both control and treated eyes, before and after treatment, are shown in Figure 7. The average ΔD, ΔR, and ΔL from the seven remaining rabbits are graphed in Figure 8 and listed individually in Table 2. With the exception of week 2 (*P* = 0.018), all time points showed significant flattening compared to baseline. Additionally, all ΔR measurements were significantly less than ΔL measurements, indicating the treated cornea was flattening at a faster rate. With the exception of one rabbit that showed a central acellular region, samples in
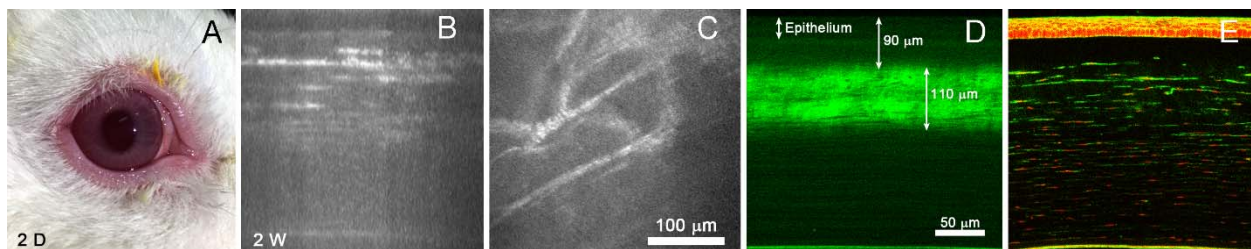

Figure 6. Short-term amplified NLO CXL. The image in (A) is a clinical image of the cornea 48 hours after treatment, showing very little irritation. (B) A representative cross-sectional reconstruction of a CMTF stack taken at 2 weeks. (C) A single-plane CMTF image, 178 μm deep, showing spindle-shaped cellular structures within the treatment region. (D) A representative CAF image showing a consistent region of CAF and an intact, regrown epithelium. (E) Cells stained with phalloidin and ethidium homodimer within the CXL region.
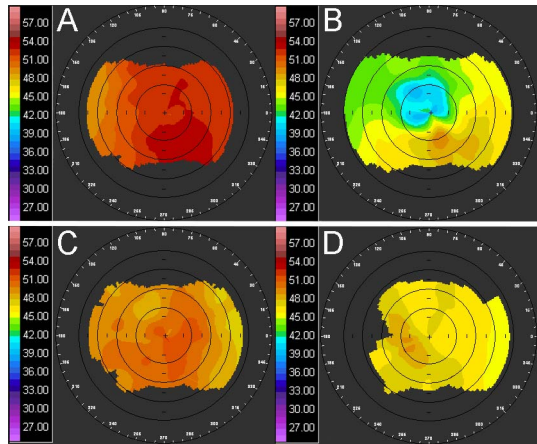
Figure 7. In vivo corneal topography. Example images of corneal topography measurements at baseline (A and C) and 2 months after treatment (B and D) of the treated right eye (A and B) and the control left eye (C and D).

which CAF was detected after 2 months showed increased cellular density throughout the crosslinked region compared to those at 2 weeks, as shown in Figure 9.

Discussion

Our previous method of NLO CXL using non-amplified FS pulses was able to produce successful crosslinking. With that system we were able to quickly scan a crosslinked volume into corneal tissue, which produced an increased corneal stiffness and blue CAF, but the average power required to do this was

Table 2. Corneal Flattening

	Time Point, wk				
	0	1	2	4	8
Total[a]					
Mean	0.1	−1.4	−0.8	−1.0	−1.2
SD	0.3	1.0	0.8	0.7	0.7
ΔR[a]					
Mean	0	−2.7[b]	−2.8[b]	−3.7[b]	−5.1[b]
SD	0	1.1	0.8	0.7	1.2
ΔL[a]					
Mean	0	−1.2	−1.9	−2.6	−3.8
SD	0	0.4	0.7	1.1	0.9

[a] Total refers to the ΔD (R-L) at each time point, ΔR refers to the R minus baseline at each time point, and ΔL refers to the L minus baseline at each time point.
[b] Refers to ΔR values, which are significantly lower than corresponding ΔL values.
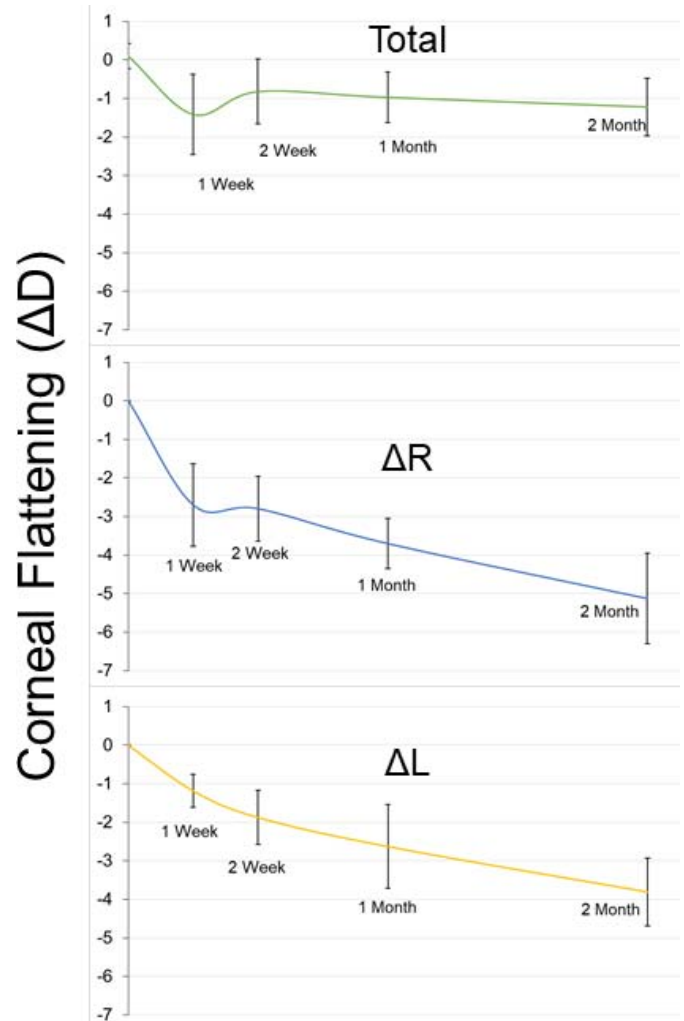

Figure 8. Amplified NLO CXL induced corneal flattening. Graph of corneal flattening measured as change in diopter of right versus left eye (Total), right eye versus baseline (ΔR), and left eye versus baseline (ΔL) over all time points. Corneal flattening decreased dramatically after 1 week of healing, then reverted slightly and began to flatten more steadily. *Error bars* represent standard deviation.

more than 17 times the ANSI limit (800 mW compared to the 46.1 mW limit).[10,11] By utilizing amplified FS pulses, we were able to design a new system that produces crosslinking using a much lower average power, remaining under the ANSI limit. This study explored the effects of amplified NLO CXL in both ex vivo and in vivo models. To our knowledge, it is the first report using amplified FS pulses for photodynamic therapy that does not involve optical breakdown.

During ex vivo experiments, it was discovered that the laser scanning speed is logarithmically related to the resulting CAF intensity. A speed of 15.5 mm/s was
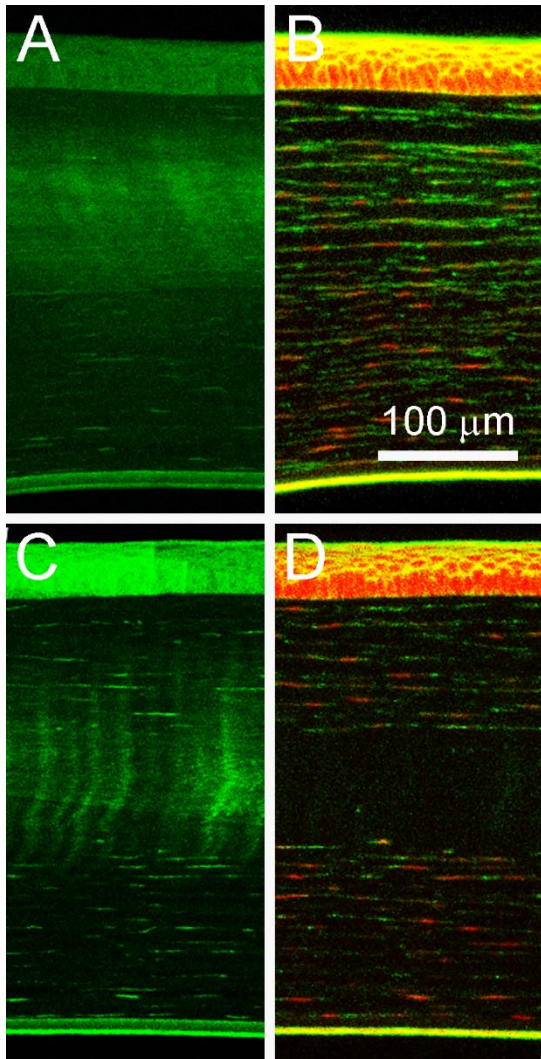
Figure 9. Long-term amplified NLO CXL. The images in (A) and (B) are representative CAF and cellular-stained images of samples after 2 months of in vivo healing. With the exception of one sample (shown in C and D), cells stained with phalloidin and ethidium homodimer had returned to the CXL region.

found to have CAF comparable to traditional UVA CXL. For this reason, the closest, easily attainable speed (20 mm/s) was used for all other experiments. We have also shown in this study that amplified NLO CXL is still capable of producing a significant increase in mechanical stiffness of corneal tissue: 1.6 times stiffer than control.

Many other studies have explored the in vivo effects of UVA CXL and found marked effects on corneal structure, specifically a flattening of at least 1 diopter lasting a year or longer.[21–25] This has increased the interest for use of corneal crosslinking to treat low refractive errors. Like UVA CXL, NLO CXL was a treatment originally designed to re-

strengthen corneas weakened by ectatic disease. This study showed that it is possible to achieve flattening with amplified NLO CXL as well, broadening the scope of this treatment to treat low refractive errors as well as corneal ectasia. Unlike UVA CXL, amplified NLO CXL has the ability to treat the cornea in a precise and customizable pattern at any depth within the cornea. For example, 50 μm below the surface was used in this study, with respect to the contact glass. With this ability it could theoretically be possible to customize corneal CXL based on individual corneal topography. Also, if riboflavin could be imbibed into the stroma without removing the epithelium, it would be possible to crosslink below the intact epithelial layer without damaging those cells during cross-linking, resulting in a more effective and less painful procedure. This study also showed repopulation of the central CXL region of treatment by keratocytes as early as 2 weeks post treatment. Our previous study has shown that this repopulation is not attained following UVA CXL out to 3 months post CXL,[13] although others have noted earlier repopulation.[26–28]

One remaining mystery left unanswered by this study is a physical explanation of why amplified FS pulses are able to produce CXL so much more efficiently than nonamplified pulses. Previous studies using nonamplified pulses had required 800 mW, 10 nJ per pulse, to produce both CAF and increased stiffening.[10,11] In these studies, the scanning speed and repetition rate were set in such a way that more than 45,000 pulses overlapped at any arbitrary volume within the treatment area. Since each individual pulse is 10 nJ, each volume would then encounter more than 450 μJ over the course of the entire treatment. As expected, no more than 8 mW of total power was needed to produce CAF using 1 μJ pulses. It had been assumed that several hundred of these pulses would need to be overlapped, but unexpectedly, the CAF spots seen in Figure 1 were created using a single pulse totaling 1 μJ, well below what was required using nonamplified pulses.

One explanation for this difference is the fluorescence lifetime of riboflavin compared to the timing of the pulses. Once a molecule of riboflavin has absorbed photons, the time it requires to pass into the excited triplet state is on the order of nanoseconds, and the half-life of the excited triplet state is around 15 μs. Any additional excitation within this half-life may be absorbed, sending the molecule back to an excited singlet state[24] and interrupting the production of free radicals entirely. The nonamplified pulse system used in our previous

studies had a repetition rate of 80 MHz, or 10 ns between pulses. This is much shorter than the half-life of the riboflavin triplet state and leaves little time for the production of oxygen free radicals. We suspect that much of the energy spent using an 80-MHz oscillator may have been wasted sending riboflavin molecules back and forth between excited singlet and triplet states without ever creating free radicals. The system used in this report had a pulse separation of 10 to 20 μs within the half-life of the riboflavin triplet state, thus creating far more energy-efficient CXL. Future experiments will be needed to test this theory.

One limitation of this study concerns measurements of corneal flattening and effects following NLO CXL. As has been noted previously, young rabbits (<6 months) as used in this study are not fully grown and show an age-related corneal flattening as well as thickening throughout their life.[29] To account for potential age-related flattening, which does not stabilize until 8 months of age,[30] each treated eye was compared to the contralateral control eye.

Another limitation of this study is the reduced measure of stiffening as compared to previous iterations of this device. While this generation of NLO CXL (using amplified pulses) was able to produce a significant 1.6 times increase in corneal elasticity, previous versions (using nonamplified pulses) and UVA CXL produced a 2.6 and 2.9 times increase, respectively, compared to control using the same indentation testing technique and equipment.[10] On its face, this difference may seem to indicate a reduced stiffening effect with amplified NLO CXL when compared to nonamplified NLO CXL or UVA CXL, but this is likely not the case for many reasons. First, amplified NLO CXL was able to induce CAF intensity levels equal to and above UVA CXL, which, according to previous studies, implies increased stiffening.[11] If amplified NLO CXL had actually produced a lower stiffening effect than did UVA CXL, it would be expected that CAF values would also be lower. Also, as stated previously, the CAF values measured in this study equaled those of previous UVA CXL studies at a speed of 15.5 mm/s. Despite this, a speed of 20 mm/s was used for convenience, which could account for a small portion of the difference. Finally, the CXL volume was both thinner (approximately half) and positioned deeper than for previous studies.[10,13] In all previous studies, mechanical measurements were performed on samples that had a CXL volume

positioned exactly at the surface of the stroma. This places the indentation needle directly in contact with the treated area. As illustrated in Figures 3, 6, and 9, the CXL volume in this study was positioned deeper into the stroma, leaving a volume of untreated tissue above. Because the indentation needle was not directly in contact with treated area during testing, the results were slightly dampened. If the speed, thickness, and depth could be adjusted to match previous reports, it is likely the results would be higher than reported in this study.

Conclusion

This study details both the development and testing of a modified NLO CXL technique. By utilizing amplified FS pulses, this technique was able to achieve both ex vivo and in vivo corneal CXL on par with nonamplified NLO CXL and traditional UVA CXL.

Acknowledgments

References

1. Wu PC, Huang HM, Yu HJ, Fang PC, Chen CT. Epidemiology of myopia. *Asia Pac J Ophthalmol (Phila)*. 2016;5:386–393.
2. Vitale S, Ellwein L, Cotch MF, Ferris FL III, Sperduto R. Prevalence of refractive error in the United States, 1999–2004. *Arch Ophthalmol*. 2008;126:1111–1119.

3. Reinstein DZ, Archer TJ, Gobbe M. The history of LASIK. *J Refract Surg*. 2012;28:291–298.

4. Solomon KD, Fernández de Castro LE, Sandoval HP, et al. LASIK world literature review: quality of life and patient satisfaction. *Ophthalmology*. 2009;116:691–701.

5. Wollensak G, Spoerl E, Seiler T. Riboflavin/ ultraviolet-A–induced collagen crosslinking for the treatment of keratoconus. *Am J Ophthalmol*. 2003;135:620–627.

6. Lim WK, Soh ZD, Choi HKY, Theng JTS. Epithelium-on photorefractive intrastromal cross-linking (PiXL) for reduction of low myopia. *Clin Ophthalmol*. 2017;11:1205–1211.

7. Wozniak KT, Gearhart SM, Savage DE, Ellis JD, Knox WH, Huxlin KR. Comparable change in stromal refractive index of cat and human corneas following blue-IRIS. *J Biomed Opt*. 2017;22:55007.

8. Chao Wang MF, Guanxiong M, Zyablitskaya M, Vukelic S. Femtosecond laser crosslinking of the cornea for non-invasive vision correction. *Nat Photonics*. 2018;12:416–422.

9. Chai D, Juhasz T, Brown DJ, Jester JV. Nonlinear optical collagen cross-linking and mechanical stiffening: a possible photodynamic therapeutic approach to treating corneal ectasia. *J Biomed Opt*. 2013;18:038003.

10. Bradford SM, Mikula ER, Chai D, Brown DJ, Juhasz T, Jester JV. Custom built nonlinear optical crosslinking (NLO CXL) device capable of producing mechanical stiffening in ex vivo rabbit corneas. *Biomed Opt Express*. 2017;8:4788–4797.

11. Bradford SM, Brown DJ, Juhasz T, Mikula E, Jester JV. Nonlinear optical corneal collagen crosslinking of ex vivo rabbit eyes. *J Cataract Refract Surg*. 2016;42:1660–1665.

12. Delori FC, Webb RH, Sliney DH; American National Standards Institute. Maximum permissible exposures for ocular safety (ANSI 2000), with emphasis on ophthalmic devices. *J Opt Soc Am A Opt Image Sci Vis*. 2007;24:1250–1265.

13. Bradford SM, Mikula ER, Juhasz T, Brown DJ, Jester JV. Collagen fiber crimping following in vivo UVA-induced corneal crosslinking. *Exp Eye Res*. 2018;177:173–180.

14. Zipfel WR, Williams RM, Webb WW. Nonlinear magic: multiphoton microscopy in the biosciences. *Nat Biotechnol*. 2003;21:1369–1377.

15. Chai D, Gaster RN, Roizenblatt R, Juhasz T, Brown DJ, Jester JV. Quantitative assessment of UVA-riboflavin corneal cross-linking using nonlinear optical microscopy. *Invest Ophthalmol Vis Sci*. 2011;52:4231.

16. Steven P, Hovakimyan M, Guthoff RF, Hüttmann G, Stachs O. Imaging corneal cross-linking by autofluorescence 2-photon microscopy, second harmonic generation, and fluorescence lifetime measurements. *J Cataract Refract Surg*. 2010;36:2150–2159.

17. Franco W, Ortega-Martinez A, Zhu H, Wang R, Irene E, Kochevar IE. Fluorescence spectroscopy of collagen crosslinking: non-invasive and in-situ evaluation of corneal stiffness. In: Larin KV, Sampson DD, eds. *Optical Elastography and Tissue Biomechanics II*, Vol. 9327. Bellingham, WA: SPIE; 2015.

18. Chai D, Gaster RN, Roizenblatt R, Juhasz T, Brown DJ, Jester JV. Quantitative assessment of UVA-riboflavin corneal cross-linking using nonlinear optical microscopy. *Invest Ophthalmol Vis Sci*. 2011;52:4231–4238.

19. Hayes WC, Keer LM, Herrmann G, Mockros LF. A mathematical analysis for indentation tests of articular cartilage. *J Biomech*. 1972;5:541–551.

20. Levental I, Levental KR, Klein EA, et al. A simple indentation device for measuring micrometer-scale tissue stiffness. *J Phys Condens Matter*. 2010;22:194120.

21. Hersh PS, Stulting RD, Muller D, Durrie DS, Rajpal RK; United States Crosslinking Study Group. United States multicenter clinical trial of corneal collagen crosslinking for keratoconus treatment. *Ophthalmology*. 2017;124:1475–1484.

22. Kanellopoulos AJ, Asimellis G. Combined laser in situ keratomileusis and prophylactic high-fluence corneal collagen crosslinking for high myopia: two-year safety and efficacy. *J Cataract Refract Surg*. 2015;41:1426–1433.

23. De Bernardo M, Capasso L, Lanza M, et al., Long-term results of corneal collagen crosslinking for progressive keratoconus. *J Optom*. 2015;8: 180–186.

24. Elling M, Kersten-Gomez I, Dick HB. Photo-refractive intrastromal corneal crosslinking for the treatment of myopic refractive errors: six-month interim findings. *J Cataract Refract Surg*. 2017;43:789–795.

25. Vinciguerra P, Albè E, Trazza S, Seiler T, Epstein D. Intraoperative and postoperative effects of corneal collagen cross-linking on progressive keratoconus. *Arch Ophthalmol*. 2009;127:1258–1265.

26. Kozobolis V, Gkika M, Sideroudi H, et al. Effect of riboflavin/UVA collagen cross-linking on central cornea, limbus and intraocular pressure.

Experimental study in rabbit eyes. *Acta Medica (Hradec Kralove)*. 2016;59:91–96.

27. Kruger A, Hovakimyan M, Ramírez Ojeda DF, et al. Combined nonlinear and femtosecond confocal laser-scanning microscopy of rabbit corneas after photochemical cross-linking. *Invest Ophthalmol Vis Sci*. 2011;52:4247–4255.

28. Wollensak G, Iomdina E, Dittert DD, Herbst H. Wound healing in the rabbit cornea after corneal collagen cross-linking with riboflavin and UVA. *Cornea*. 2007;26:600–605.

29. Doughty MJ. The cornea and corneal endothelium in the aged rabbit. *Optom Vis Sci*. 1994;71: 809–818.

30. Riau AK, Tan NY, Angunawela RI, Htoon HM, Chaurasia SS, Mehta JS. Reproducibility and age-related changes of ocular parametric measurements in rabbits. *BMC Vet Res*. 2012;8:138.

translational vision science & technology